OPEN

Citation: Cell Death and Disease (2014) 5, e1050; doi:10.1038/cddis.2014.4
© 2014 Macmillan Publishers Limited All rights reserved 2041-4889/14
www.nature.com/cddis

miR-542-3p suppresses osteoblast cell proliferation and differentiation, targets BMP-7 signaling and inhibits bone formation

J Kureel[1], M Dixit[1], AM Tyagi[1], MN Mansoori[1], K Srivastava[1], A Raghuvanshi[2], R Maurya[2], R Trivedi[1], A Goel[2] and D Singh*[,1]

MicroRNAs (miRNAs) are short non-coding RNAs that interfere with translation of specific target mRNAs and thereby regulate diverse biological processes. Recent studies have suggested that miRNAs might have a role in osteoblast differentiation and bone formation. Here, we show that miR-542-3p, a well-characterized tumor suppressor whose downregulation is tightly associated with tumor progression via C-src-related oncogenic pathways, inhibits osteoblast proliferation and differentiation. miRNA array profiling in Medicarpin (a pterocarpan with proven bone-forming effects) induced mice calvarial osteoblast cells and further validation by quantitative real-time PCR revealed that miR-542-3p was downregulated during osteoblast differentiation. Over-expression of miR-542-3p inhibited osteoblast differentiation, whereas inhibition of miR-542-3p function by anti-miR-542-3p promoted expression of osteoblast-specific genes, alkaline phosphatase activity and matrix mineralization. Target prediction analysis tools and experimental validation by luciferase 3′ UTR reporter assay identified BMP-7 (bone morphogenetic protein 7) as a direct target of miR-542-3p. It was seen that over-expression of miR-542-3p leads to repression of BMP-7 and inhibition of BMP-7/PI3K- survivin signaling. This strongly suggests that miR-542-3p suppresses osteogenic differentiation and promotes osteoblast apoptosis by repressing BMP-7 and its downstream signaling. Furthermore, silencing of miR-542-3p led to increased bone formation, bone strength and improved trabecular microarchitecture in sham and ovariectomized (Ovx) mice. Although miR-542-3p is known to be a tumor repressor, we have identified second complementary function of miR-542-3p where it inhibits BMP-7-mediated osteogenesis. Our findings suggest that pharmacological inhibition of miR-542-3p by anti-miR-542-3p could represent a therapeutic strategy for enhancing bone formation *in vivo*.

Cell Death and Disease (2014) **5,** e1050; doi:10.1038/cddis.2014.4; published online 6 February 2014
Subject Category: Experimental Medicine

MicroRNAs (miRNAs) are an abundant class of evolutionarily conserved, small (~22 nucleotides), single-stranded non-coding RNAs found in diverse organisms. These have emerged as an important post-transcriptional regulators of gene expression.[1–6] They negatively regulate translation of specific mRNAs by base pairing with partially or fully complementary sequences in target mRNAs.[1–6] Although the biological functions of most miRNAs are not yet fully understood, they may have a key role in the regulation of various biological processes, including developmental timing, cellular differentiation, proliferation, apoptosis, gene regulation, insulin secretion, cholesterol biosynthesis and cancer development.[1,3,4,6,7] An increasing number of miRNAs have been identified to regulate osteoblast differentiation and bone formation positively by targeting negative regulators of osteogenesis or negatively by targeting important osteogenic factors.[1,2,4–6,8–10] Several studies have demonstrated that miRNAs target the principal transcription factors and signaling molecules involved in osteoblast differentiation of MSCs and osteoblast functions.[11] miRNAs 133 and 204/211 attenuated osteoblast differentiation by directly targeting Runx2 in C2C12 mesenchymal progenitor cells and MSCs, respectively.[12,13] miRNAs miR-141 and miR-200a were downregulated during pre-osteoblast differentiation and inhibited osteoblastogenesis by targeting Dlx5.[14] miR-335-5p was shown to directly target and downregulate Wnt inhibitor DKK1, enhance Wnt signaling and promote osteogenesis.[15] A novel miRNA, miR-2861, was identified by Li *et al.*[6] to contribute to osteoporosis in mice and humans. miRNAs may thus represent novel therapeutic targets for pharmacological control of bone cell functions and enhancement of bone formation.

Several studies have focused on miRNAs modulated by bone morphogenetic protein (BMP) signaling as a means to understand the role of miRNAs in osteoblasts.[6,12,16] These studies have shown that a number of BMP-regulated miRNAs are important for the regulation of osteoblast differentiation.[6,12,17] Previous studies by our group have shown that Medicarpin, a pterocarpan, stimulates osteoblast differentiation by ER-BMP-2 pathway.[18] As Medicarpin (Med) stimulated BMP-2 signaling, which downregulates several

[1]Division of Endocrinology and Centre for Research in Anabolic Skeletal Targets in Health and Illness (ASTHI), Lucknow, India and [2]Division of Medicinal & Process Chemistry, CSIR-Central Drug Research Institute, B.S. 10/1, Sector-10, Jankipuram Extension, Lucknow, India
*Corresponding author: D Singh, Division of Endocrinology and Centre for Research in Anabolic Skeletal Targets in Health and Illness (ASTHI), B.S.10/1, Sector-10, Jankipuram Extension, Lucknow, Uttar Pradesh 226031, India. Tel: +91 522 2772550 Ext: 4395; Fax: +91 522 2771940; E-mail: divya_singh@cdri.res.in
Keywords: microRNAs; osteoblast differentiation; proliferation; bone formation; bone strength; trabecular microarchitecture
Abbreviations: MiRNA, microRNA; BMP, bone morphogenetic protein; OCN, osteocalcin; ALP, alkaline phosphatase; BFR, bone formation rate; MAR, mineral appositional rate
Received 26.7.13; revised 12.12.13; accepted 13.12.13; Edited by G Melino

miRNA candidates known to target various osteogenic pathways, we speculated that changes in miRNA expression may have a role in osteogenic effects of Med. Using Med-induced osteogenesis from primary calvarial-derived osteoblast cells, miRNA profiling was done which showed upregulation of a limited cohort of miRNAs that have predicted targets for Brca 1, IL-1receptor type 1, Interleukin7, interleukin enhancer binding factor 3 and Brca1-associated protein 1. About 80 miRNAs were downregulated in response to the Medicarpin treatment. Majority of these miRNAs had predicted targets that are positive regulators of bone formation, including mediators of the Wnt and BMP and transcriptional regulators of osteogenesis. Of the various candidates, one miRNA of potential interest was miR-542-3p. miR-542-3p has been well studied for its role as a tumor suppressor where its downregulation is tightly associated with tumor progression via C-src-related oncogenic pathways.[19,20] However, our studies show that miR-542-3p has a complementary role in osteoblast differentiation where it suppresses osteogenesis. By modulating miR-542-3p activity, we show that inhibition of miR-542-3p by an anti-miR markedly increased osteogenic proliferation and differentiation *in vitro*, inhibited osteoblast apoptosis and enhanced bone formation *in vivo*. BMP-7 was identified as a direct target of miR-542-3p. It was observed that inhibition of miR-542-3p by anti-miR-542-3p represses BMP-7 and blocks the BMP-7/PI3K- survivin signaling that coincides with increased bone formation. This strongly suggests that miR-542-3p suppresses osteogenic differentiation and promotes osteoblast apoptosis by repression of BMP-7 and its downstream signaling. Overall, our studies support a previously uncharacterized function for miR-542-3p wherein it participates in the inhibition of osteoblast functions and bone formation *in vivo*.

Results

Identification of miRNAs with differential expression during Med-induced osteoblast differentiation. To study the expression of miRNAs whose expression was altered during Med-induced osteoblast differentiation, calvaria-derived primary osteoblast cells were treated with Med for 48 h. At this time point, Med maximally induced the expression of osteogenic gene markers such as alkaline phosphatase (ALP), BMP-2, BMP-7, Type I col, osteocalcin (OCN), RUNX2 and Osx (Supplementary Figure S1). Cells treated with or without Med were subjected to microarray analysis. Osteoblasts express many miRNAs, and most of the miRNAs were downregulated by Med treatment, whereas only a few of them were upregulated. Of these, the most interesting was miR-542-3p as its expression was significantly downregulated during osteoblast differentiation (Figure 1a). Moreover miR-542-3p is an established tumor suppressor;[19] however, its role in osteoblast differentiation has never been explored. These data were further verified by quantitative real-time PCR (qRT-PCR) in the mice osteoblast cells. It was observed that expression of miR-542-3p was significantly downregulated in Med-treated osteoblast cells (Figure 1b). Importantly, miR-542-3p expression was also suppressed in BMP-2-treated osteoblast cells (Figure 1b).

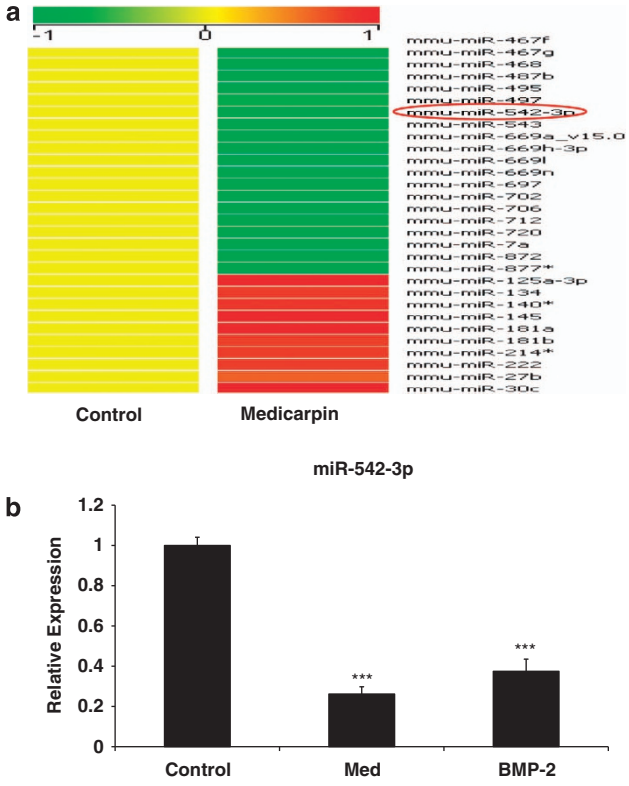

Figure 1 Identification of miRNAs with differential expression during Med-induced osteoblast differentiation. Cells were treated with Med at 100 pM concentration for 48 h in α-MEM supplemented with 5% FCS, 10 mM β-glycerophosphate, 50 μg/ml ascorbic acid and 1% penicillin/streptomycin. (**a**) miRNA array expression profiling. Red denotes high expression and green denotes low expression relative to the median and only representative miRNAs that were significantly downregulated and upregulated are shown. (**b**) miR-542-3p expression during Med- and BMP-2-induced murine osteoblast differentiation. All values represent means ± S.E. ($n=6$). $^{**}P<0.01$, $^{***}P<0.001$ compared with the control

miR-542-3p regulates osteoblast differentiation. To evaluate the effect of miR-542-3p on osteoblast differentiation, osteoblast cells were transfected with 50 nM of miR-C, 50 nM of mimic miR-542-3p and 20 nM of anti-miR-542-3p and induced to differentiation in growth medium containing 10 mM β-glycerophosphate and 50 μg/ml ascorbic acid. ALP activity, one of the major osteoblast differentiation marker, was measured after 48 h. Compared with cells transfected with miR-C, ALP activity was significantly downregulated in miR-542-3p-transfected cells, whereas this effect was attenuated in anti-miR-542-3p-transfected cells (Figure 2a). Following this, effect of miR-542-3p was seen on mineral nodule formation by alizarin staining which can be used to visually detect the presence of mineralization in bone tissue as it binds with the calcium in mineralized matrix. As shown in Figure 2b, transfection of miR-542-3p decreased the mineralized nodule formation in 21-day culture. However, this effect was blocked in anti-miR-542-3p-transfected cells. Transfection of mimic miR-542-3p also inhibited the expression of osteogenic gene markers such as RUNX2, BMP2, Type I col, Osx and OCN (Figure 2c). This effect was abolished in anti-miR-542-3p-transfected cells. Interestingly,

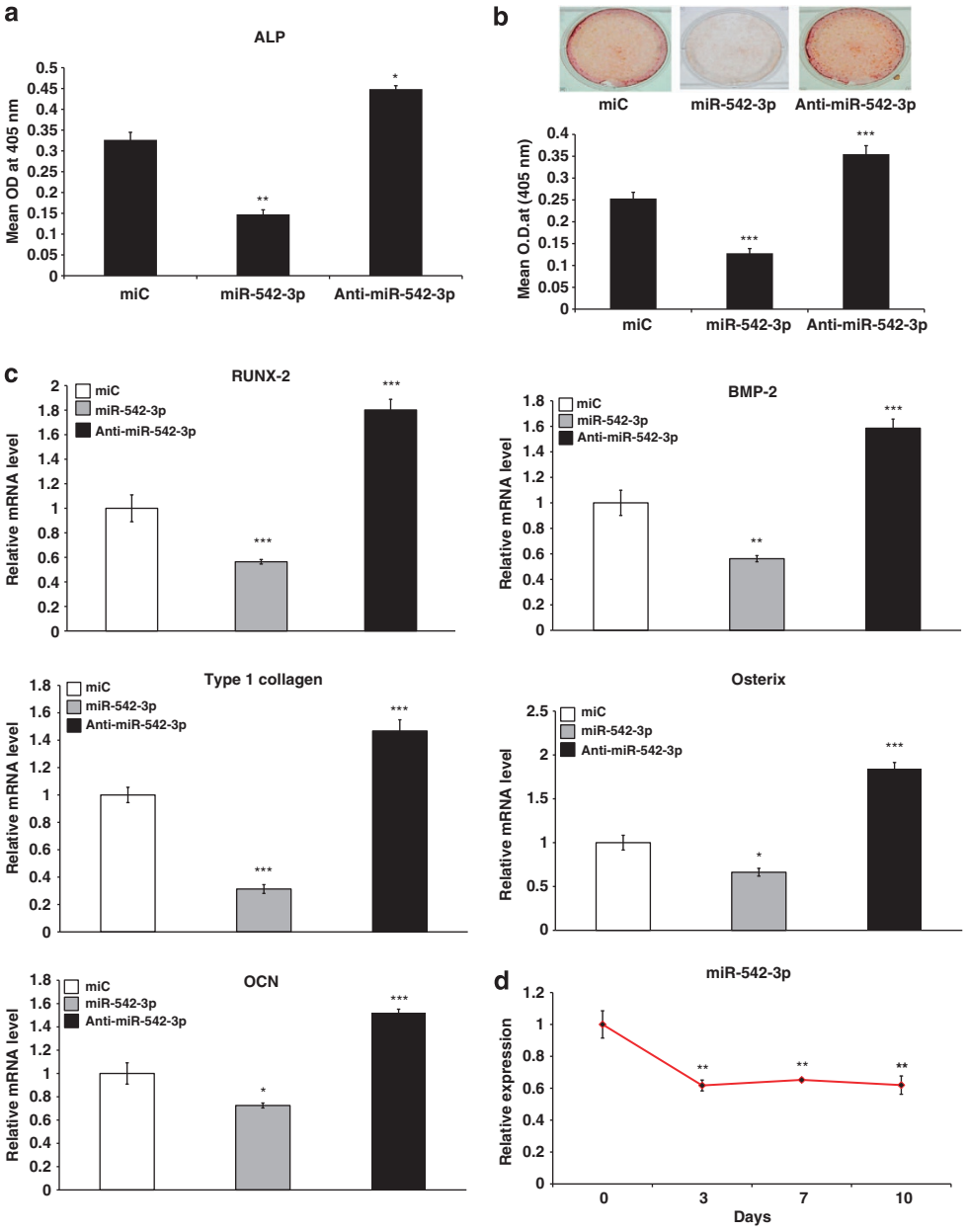

Figure 2 miR-542-3p regulates osteoblast differentiation. (**a**) Murine calvarial osteoblasts were transfected with miC, miR-542-3p and anti-miR-542-3p for 48 h in differentiation medium (growth medium containing ascorbic acid and β-glycerophosphate). ALP activity in murine osteoblasts was measured. (**b**) Murine osteoblasts were (2.5×10^3cells/well) seeded in 12-well plates and cultures were continued for 21 d followed by staining with alizarin red-S. Representative photomicrographs show mineralized nodules in different groups. Stain was extracted and quantified. (**c**) qRT-PCR analysis of osteoblast marker genes (RUNX-2, BMP-2, Type 1 collagen, OSX, OCN normalized to GAPDH) at 48 h. (**d**) Change in miR-542-3p expression during osteoblast differentiation. All values represent means ± S.E. ($n = 6$). $^*P < 0.05$, $^{**}P < 0.01$, $^{***}P < 0.001$ compared with the miR-542-3p and anti-miR-542-3p

it was seen that miR-542-3p expression decreased during the course of osteoblast differentiation (Figure 2d). In addition, miR-542-3p was transfected in human osteoblast cells (hOB) and it was observed that miR-542-3p over-expression leads to decreased ALP activity and transcript levels of osteogenic markers like RUNX2, Type I col, Osx and OCN. This effect was reversed in hOB transfected with anti-miR-542-3p (Supplementary Figure S2). All of these results suggest that miR-542-3p negatively regulates osteoblast differentiation.

miR-542-3p directly targets BMP-7. We next studied the molecular mechanism by which miR-542-3p regulates osteoblast functions. Target prediction tools TargetScan (http://www.targetscan.org), PicTar (http://pictar.mdc-berlin.de/) and microRNA.org (http://www.microrna.org) were utilized in order to find out possible target genes for miR-542-3p. Among the many genes that were predicted to be the potential targets by both databases, we focused on BMP-7, a member of the TGF-β super family that has a major role in osteoblast differentiation and function.[21–23] Using target

prediction tools, it was found that miR-542-3p targets in the 3′ UTR of BMP-7 (Figure 3a). To test whether miR-542-3p can directly regulate BMP-7, a luciferase reporter construct containing the 3′ UTR of BMP-7 was used. In addition, a luciferase reporter construct containing mutations in the 3′ UTR of BMP-7 was also synthesized. The wild-type and mutant BMP-7 luciferase expression vectors were transfected with mimic miR-542-3p in calvarial osteoblast cells and the level of luciferase enzyme activity was measured. Over-expression of miR-542-3p suppressed the luciferase activity of the reporter gene (Figure 3b). Mutation of two nucleotides within the miRNA binding site abolished this repression of luciferase activity confirming the specificity of the action (Figure 3b). To directly test the validity of the putative target, calvarial osteoblast cells were transfected with mimic miR-542-3p. The mRNA level of BMP-7 was measured by qRT-PCR. Relative to the control, over expression of miR-542-3p downregulated BMP-7 mRNA (Figure 3c).

miR-542-3p regulates BMP-7-mediated PI3K/survivin pathway thereby enhancing osteoblast apoptosis. BMP-7 which was originally identified as osteogenic factor also has important roles in multiple cellular processes such as cell growth, differentiation, apoptosis and in cancer.[24] BMP-7 has been shown to induce PI3K/Akt pathway to inhibit granulosa cell apoptosis.[25] Both BMP-7 and PI3K/Akt activation induces the expression of survivin,[26,27] a member of the inhibitor of apoptosis family and miR-542-3p is known to reduce both mRNA and protein levels of survivin.[20] Western blot analyses show that transfection with mimic miR-542-3p reduced protein levels of BMP-7 and inhibited the phosphorylation of Akt and survivin (Figure 4a). This effect was blocked in cells transfected with anti-miR-542-3p (Figure 4a). As survivin inhibits apoptosis through the caspase enzyme system,[28] protein levels of caspase 3 were also measured. Western blot analysis shows that transfection with miR-542-3p led to increased levels of caspase 3 (Figure 4a) while anti-miR-542-3p reversed this effect (Figure 4a). Increased caspase 3 is an indicator of apoptosis, hence calvarial osteoblasts were transfected with miR-542-3p and anti-miR-542-3p and apoptosis in cells was assessed by FACS using Annexin-PI staining. miC was used as a control. We observed that osteoblasts transfected with miR-542-3p had 20.84% apoptotic cells, while this percentage of apoptotic cells was significantly brought down to 3.63% in

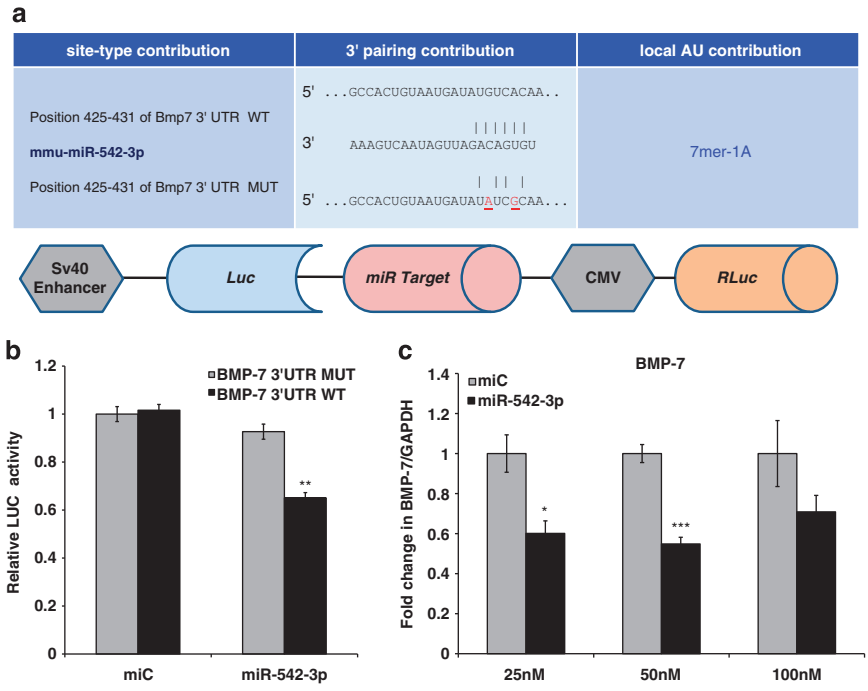

Figure 3 Identification of miR-542-3p target genes in osteoblast differentiation. (**a**) Computational analysis was performed for the complementarities of miR-542-3p to the 3′ UTR of BMP-7 and schematic presentation of the reporter plasmid used to illustrate the effect of BMP-7 3′ UTR on luciferase activity. CMV, cytomegalovirus promoter; Luc, luciferase. (**b**) Effect of miR-542-3p over-expression on a dual luciferase reporter plasmid containing the BMP-7 3′ UTR was analyzed. Cells were co-transfected with either the WT-pEZX MT01-BMP7 or MUT-pEZX MT01-BMP7 or an empty vector and miR-542-3p or miC. Firefly and renilla luciferases were measured in cell lysate. (**c**) Cells were transfected with the miR-542-3p expression plasmid or a control. qRT-PCR analysis for BMP-7 expression was performed. GAPDH was used as an internal control

Figure 4 MiR-542-3p regulates BMP-7-mediated PI3K/survivin pathway and enhances osteoblast apoptosis. (**a**) Western blot analysis for BMP-7, Akt/p-Akt, Survivin/pSurvivin and caspase3 protein was performed from cell lysate collected at 48 h after transfection with miC, miR-542-3p and anti-miR-542-3p. β-Actin was used as an internal control. (**b**) MiR-542-3p enhances osteoblast apoptosis, an effect reversed by anti-miR-542-3p. Representative images of FACS analysis using staining with annexin and propidium iodide (PI) in miC, miR-542-3p- and anti-miR-542-3p-transfected osteoblast cells. % of apoptotic cells as analyzed by FACS. All values represent means ± S.E. ($n=4$). *$P<0.05$, **$P<0.01$, ***$P<0.001$ compared with the counterparts shown

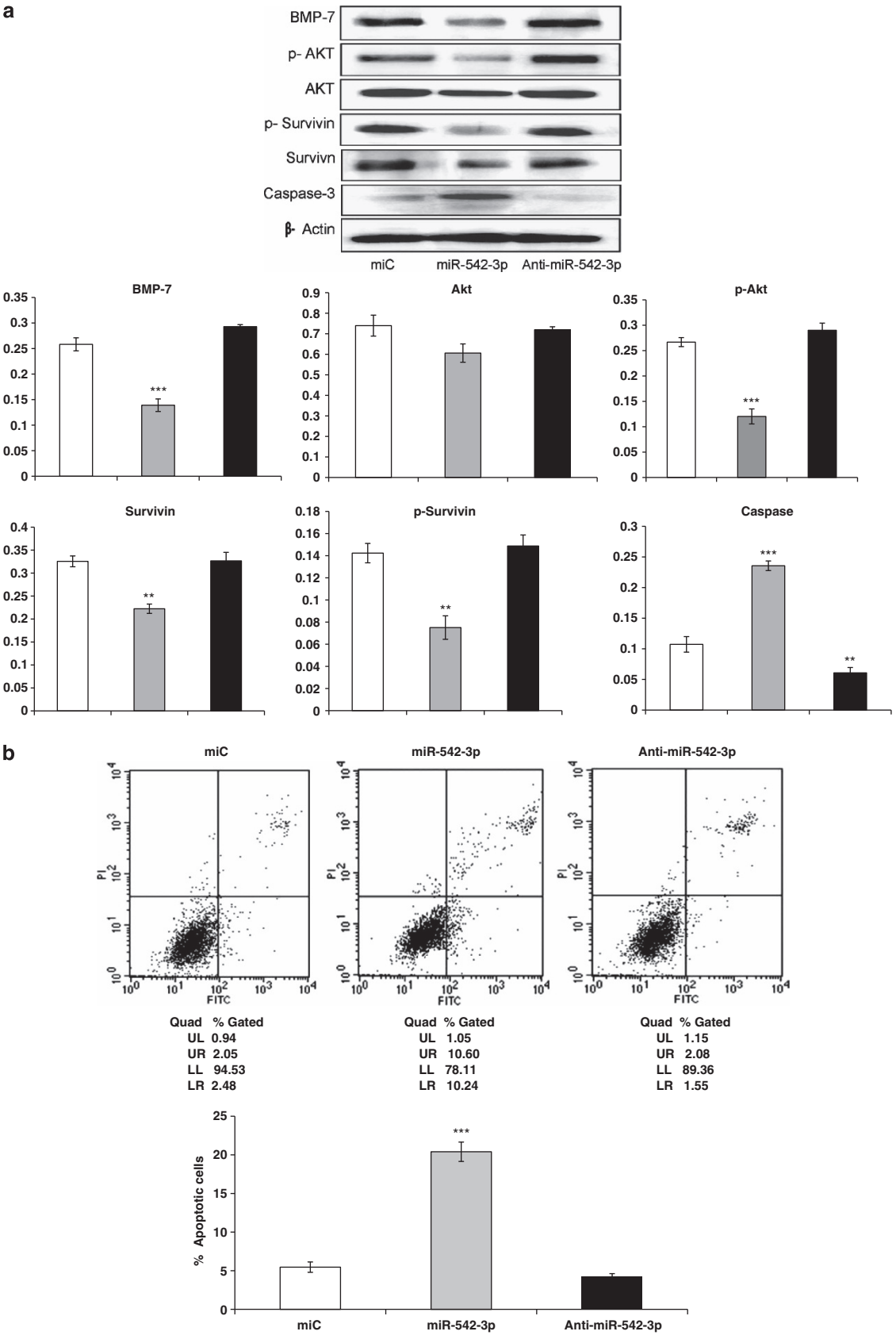
a
BMP-7
p- AKT
AKT
p- Survivin
Survivn
Caspase-3
β- Actin
miC
miR-542-3p
Anti-miR-542-3p
BMP-7
Akt
p-Akt
Survivin
p-Survivin
Caspase
b
miC
miR-542-3p
Anti-miR-542-3p
PI
FITC
Quad % Gated
UL 0.94
UR 2.05
LL 94.53
LR 2.48
Quad % Gated
UL 1.05
UR 10.60
LL 78.11
LR 10.24
Quad % Gated
UL 1.15
UR 2.08
LL 89.36
LR 1.55
% Apoptotic cells
miC
miR-542-3p
Anti-miR-542-3p

anti-miR-542-3p-transfected cells (Figure 4b). These data indicate that miR-542-3p induces apoptosis in osteoblast cells while anti-miR-542-3p abolishes this effect. In addition, over-expression of miR-542-3p inhibited osteoblast cell proliferation, an effect that was reversed by anti-miR-542 3p transfection (Supplementary Figure S3). Thus, overall miR-542-3p inhibits BMP-7-mediated PI3K/survivin, non-smad pathway thereby leading to decreased osteoblast proliferation and increased osteoblast apoptosis.

miR-542-3p regulates bone formation *in vivo*. To investigate the function of miR-542-3p *in vivo*, we performed an experiment in which a chemically modified antisense oligonucleotide specific to miR-542-3p (*In vivo* ready miRNA inhibitor of miR-542-3p obtained from Life Technologies (Carlsbad, CA, USA)) was injected at 7 mg/kg body weight dose[29] via a single tail vein injection into mice that had undergone sham operation or ovariectomy (Ovx). miC (7 mg/kg body weight dose) and PBS (0.2 ml) were used as controls. Mice were treated with miR-542-3p inhibitor for 3 consecutive days in the first week followed by another injection on days 1–3 of the fourth week. Study plan is given in Figure 5a. All mice were euthanized for analysis by the end of the sixth week after the first injection. Quantification of the bone volume/tissue volume ratio (BV/TV), trabecular number (Tb.N), trabecular spacing (Tb.Sp) and trabecular thickness (Tb.Th) was conducted using micro-CT. The representative micro-CT images are shown in Figure 5b. Quantification of micro-CT data revealed that miR-542-3p inhibitor-treated sham mice show significantly increased bone parameters, including BV/TV, Tb.N and Tb.Th, with a concomitant decrease in Tb.Sp in femora, tibial and vertebral bones (Figures 5c–e). Ovx mice treated with miR-542-3p inhibitor also exhibited a significant increase in BV/TV, Tb.N and Tb.Th and decrease in Tb.Sp (Figures 5c–e). Besides, miR-542-3p inhibitor-treated Ovx mice exhibited significant reduction in bone turnover markers like serum OCN and serum CTx (Supplementary Figures S4a and b). Results showed that in sham groups, miR-542-3p inhibitor-treated mice exhibited increased bone formation rate (BFR) and mineral appositional rate (MAR). A significant increase in these bone formation parameters was also detected in Ovx mice treated with miR-542-3p inhibitor (Figure 5f). Representative images are shown in Supplementary Figure S5. We also performed biomechanical testing on mouse femur and fifth vertebra. miR-542-3p inhibitor treatment to Ovx mice increased biomechanical index value, such as ultimate force, energy and stiffness (Table 1). These values were further increased in miR-542-3p inhibitor-treated Sham mice (Table 1). These results suggested that miR-542-3p is involved in the regulation of bone metabolism.

Discussion

In the present study, we identified what is to our knowledge an uncharacterized function of miR-542-3p, which inhibits bone formation by repressing BMP-7 expression. Previous studies have shown that downregulation of miR-542-3p is tightly associated with tumor progression via c-Src-related oncogenic pathways.[19] Human cancer cells over-expressing c-Src have levels of miR-542-3p substantially downregulated, and the ectopic expression of miR-542-3p suppresses tumor growth.[19] Besides, miR-542-3p reduces mRNA and protein levels of survivin, an apoptosis inhibitor.[20] Thus, role of miR-542-3p as a tumor suppressor is well established. However, our study reports a novel function of miR-542-3p wherein over-expression of miR-542-3p critically regulates bone metabolism, and this regulation is mostly through its function in osteoblast.

Studies carried out by our group had previously shown that Med induces osteogenesis by BMP-2 signaling pathway.[18] As BMP-2 regulates several miRNA candidates known to target various osteogenic pathways,[21,22] hence, osteoblast cells were stimulated with Med to study differentially regulated miRs. Of the various candidates, miR-542 3p was chosen as it was significantly downregulated in Med-stimulated osteoblast cells and also owing to its role as a tumor suppressor. The expression of miR-542-3p was also validated by determining its expression in Med- and BMP-2-treated osteoblast cells. It was observed that stimulation of osteoblast differentiation with Med or BMP-2 led to significant repression of miR-542-3p.

To determine whether miR-542-3p directly regulates osteoblast differentiation, we investigated the action of miR-542-3p in the process of osteoblastogenesis. MiR-542-3p over-expression inhibited osteoblast differentiation. In contrast, over-expression of anti-miR-542-3p increased osteoblast differentiation as assessed by ALP. MiR-542-3p over-expression also decreased the mineral nodule formation and led to downregulation of several osteogenic markers like Runx-2, BMP-2, Type I col and Osx mRNA levels, an effect that was abolished by anti-miR-542-3p treatment. Role of miR-542-3p was also validated in hOB where its over-expression led to decreased ALP activity and diminished mRNA levels of osteogenic gene markers.

To study the molecular mechanism by which miR-542-3p regulates osteoblastogenesis, we searched for potential target genes that have an established function in promoting osteogenesis using target prediction tools like pictar and target scan. Interestingly, it was observed that the miR-542-3p targets the 3′ UTR of BMP-7. BMP-7 has a key role in the transformation of mesenchymal cells to bone and cartilage.[30] It induces the phosphorylation of Smad1/5, essential for the activation of bone-specific genes.[31] Using a luciferase BMP-7 3′ UTR reporter gene, we show that over-expression of mimic miR-542-3p suppressed the luciferase activity of the reporter construct. However, this effect was abolished when luciferase reporter containing a mutant 3′ UTR of BMP-7 was co-transfected with mimic miR-542-3p, thus confirming the specificity of action. This was further validated when decreased levels of BMP-7 mRNA was observed in cells transfected with miR-542-3p.

As one of the targets of miR-542-3p is survivin, a member of inhibitor of apoptosis protein which inhibits apoptosis through the caspase enzyme system[28] and there are reports that survivin promotes osteoblast cell proliferation and survival,[32] it was of interest to see the effect of miR-542-3p over-expression on osteoblast proliferation and survival. Moreover, there are reports that BMP-7 protects prostate cancer cells from stress-induced apoptosis by survivin induction and also

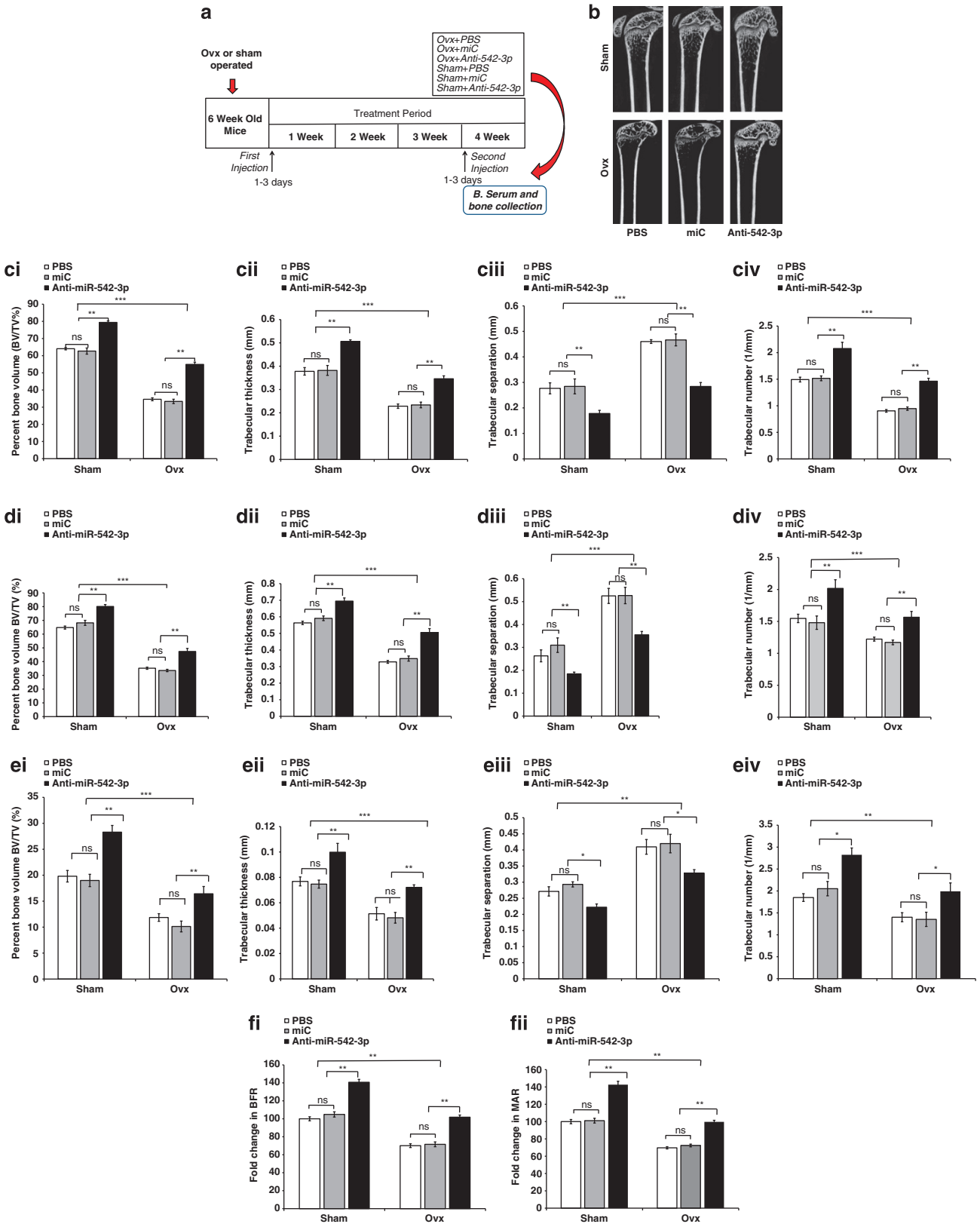

Figure 5 MiR-542-3p is a regulator of bone formation *in vivo*. (**a**) A schematic diagram illustrating the experimental setup. (**b**) Representative 2D images of distal femur. (**c**) Anti-miR-542-3p restores tibial microarchitecture showing BV/TV, bone volume/tissue volume (%); Tb.N, trabecular number (1/mm); Tb.Th, trabecular thickness (mm); and Tb.Sp, trabecular spacing (mm). (**d**) Anti-miR-542-3p restores femoral microarchetecture and (**e**) vertebral microarchetecture. (**f**) Analysis of cortical periosteal histomorphometric parameters (MAR and BFR/BS) in femur. All values represent means ± S.E. ($n=8$). *$P<0.05$, **$P<0.01$, ***$P<0.001$ compared with the counterparts shown

Table 1 Effect of miC and anti-miR-542-3p on bio-mechanical properties of isolated femur and fifth lumbar vertebrae

Treatment	Dose (mg/kg)	Bending force, right femur bone		Compression, fifth vertebrae (LV5)	
		Ultimate force (N)	Stiffness (N/mm)	Energy (mJ)	Stiffness (N/mm)
Sham + PBS	–	24.00 ± 0.87	74.720 ± 2.12	239.8 ± 3.17	490.63 ± 15.76
Sham + miC	07	22.70 ± 1.06	73.470 ± 0.80	347.5 ± 5.34	368.86 ± 18.49
Sham + Anti-miR-542-3p	07	27.3^{g} ± 0.26	90.67^{g} ± 2.80	405.1^{g} ± 2.62	634.80^{h} ± 87.47
Ovxe + PBS	–	17.700 ± 0.28	37.500 ± 1.11	239.300 ± 9.10	265.630 ± 11.32
Ovx + miC	07	18.300^{c} ± 0.76	36.97^{c} ± 2.61	256.10^{c} ± 5.55	291.07^{d} ± 07.80
Ovx + Anti-miR-542-3p	07	$22.00^{e,a}$ ± 0.50	$59.10^{e,a}$ ± 2.61	$335.6^{e,a}$ ± 6.55	$404.63^{f,b}$ ± 03.36

Values represent mean ± S.E.M. of at least 8 observations in each treatment group
$^{h}P<0.01$, $^{g}P<0.001$; Sham miC *versus* Sham anti-miR-542-3p group
$^{b}P<0.01$, $^{a}P<0.001$; Ovx miC *versus* Ovx anti-miR-542-3p group
$^{d}P<0.05$, $^{c}P<0.001$; Sham miC *versus* Ovx miC group
$^{f}P<0.01$, $^{e}P<0.001$; Sham anti-miR-542-3p *versus* Ovx anti-miR-542-3p group
All other relevant comparisons were statistically non-significant

suppresses granulosa cell apoptosis via PI3K/PDK-1/Akt pathway which in turn also induces survivin.[25–27] Thus, the effect of miR-542-3p was studied on protein levels of BMP-7, Akt, survivin and caspase 3. It was observed that in miR-542-3p-treated cells, BMP-7 protein levels and phosphorylation of Akt and survivin was suppressed leading to caspase 3 activation which may then enhance osteoblast apoptosis. This was confirmed when miR-542-3p-transfected osteoblast cells were assessed for apoptosis by FACS using Annexin-PI staining. Although increased percentage of apoptotic cells were observed in miR-542-3p-transfected cells, this effect was reversed in anti-miR-542-3p-transfected osteoblasts. Thus, we propose that miR-542 3p may inhibit osteoblast proliferation and survival via BMP-7/PI3K-survivin non-smad pathway and osteoblast differentiation via smad pathway (Figure 6). This may lead to an inhibition of osteoblast proliferation, survival and differentiation by miR-542-3p.

As miR-542-3p-suppressed osteoblast proliferation and differentiation *in vitro*,[25–27] it may have an important role in bone formation *in vivo*. Thus, we used *in vivo* ready miRNA inhibitor against miR-542-3p so that it can be silenced endogenously with high efficiency and specificity in mice. For this study, Ovx mice model was used as this model correctly emulates the important clinical feature of the estrogen-depleted human skeleton and the response of therapeutic agents.[33] Mice lacking miR-542-3p were generated through intravenous administration of miR-542-3p inhibitor. Our results showed that silencing of miR-542-3p led to an increase in bone mass in sham mice and enhanced bone mass gain in Ovx mice. Bone turnover markers like serum OCN and serum CTx were significantly reduced in Ovx animals treated with miR-542-3p inhibitor with no effect in sham group. Silencing of miR-542-3p also led to significant improvement in trabecular microarchitecture in Ovx animals. In fact, silencing of miR-542-3p led to an even enhanced effect on the trabecular architecture in sham animals. These data suggest that miR-542-3p regulates bone formation.

In conclusion, we find that miR-542-3p functions as a negative regulator of osteogenesis by repressing BMP-7 expression, which in turn, may result in suppression of smad-dependent and non-smad BMP-7/PI3K-Survivin signaling pathway. Importantly, our results show that functional inhibition of miR-542-3p can accelerate osteoblast proliferation and differentiation and lead to increased bone formation *in vivo*. As miR-542-3p exerts a negative regulatory role in human osteoblasts also, hence, we propose that therapeutic approaches targeting miR-542-3p could be useful in enhancing the bone formation and treatment of pathological conditions of bone loss.

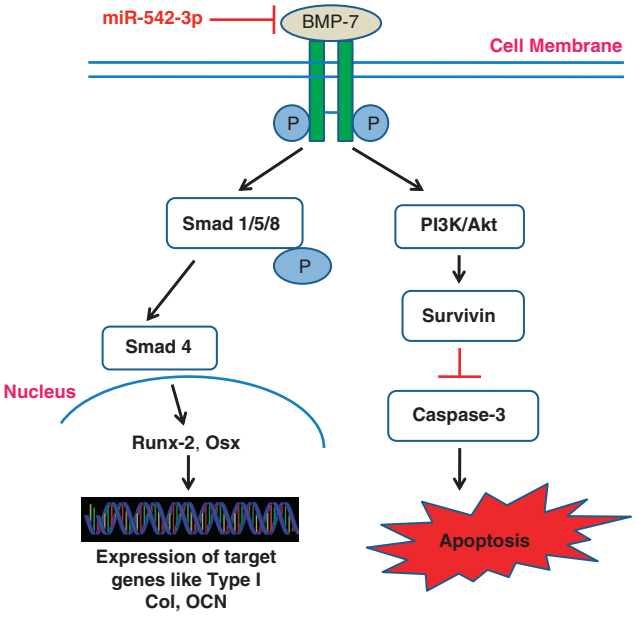

Figure 6 A proposed model for miR-542-3p-mediated suppression of osteoblast proliferation and differentiation. miR-542-3p suppresses BMP-7 translation, thereby decreasing the phosphorylation of Akt and survivin which leads to caspase-3 activation and increased osteoblast apoptosis. It also decreases osteoblast differentiation by smad-dependent pathway thereby suppressing the expression of master transcription factors like Runx-2 and OSX and inhibiting bone formation

Materials and Methods

***In vitro* bone formation using osteoblast culture.** Mouse calvarial osteoblasts were obtained following our previously published protocol of sequential digestion.[34–37] Calvariae were subjected to five sequential digestions at 37 °C in 0.1% dispase and 0.1% collagenase P solution. Cells released from the second to fifth digestions were collected, pooled, centrifuged, resuspended and plated in

T-25cm2 flasks in α-MEM media containing 10% fetal calf serum (FCS) and 1% penicillin/streptomycin. Human osteoblast cells (procured from European collection of cell cultures (ecacc), UK) were maintained in α-MEM media containing 10% FCS and 1% penicillin/streptomycin.

miRNA microarray and data analysis. Microarray procedure was performed at Genotypic Pvt. Ltd in a protocol using Agilent miRNA Hybridization kit. Briefly 100 ng of total RNA was dephosphorylated with calf intestinal alkaline phosphatase, followed by denaturing with 100% dimethyl sulfoxide at 100 °C. The method involved the ligation of one cyanine-3-pCp molecule to the 3' end of dephosphorylated single-stranded RNA (including miRNA) by T4 RNA ligase with $>$90% efficiency. The labeled miRNA were hybridized to mouse miRNA 8 $\times$ 15K microarrays in a rotating hybridization oven at 10 rpm for 20 h at 55 °C followed by sequential washing in Agilent GE Wash Buffer 1 with Triton X-102 and Agilent GE Wash Buffer 2 with Triton X-102. After washing, all slides were immediately scanned at 5 μm resolution in a green dye channel by using Agilent microarray scanner. Feature Extraction software was used to quantify the scanned images. The differentially expressed miRNAs were identified by using a standard protocol developed for mRNA gene arrays.

miRNA target site prediction. Target prediction tools Target Scan (http://www.targetscan.org), PicTar (http://pictar.bio.nyu.edu) and miRanda (http://www.microrna.org) were utilized in order to find out possible target genes for the differentially expressed miRNAs. Computational target prediction is primarily based on potential pairing of the miRNA seed sequence to a complementary site in the 3′ UTR of a target mRNA according to specific base-pairing rules.

qRT-PCR analysis for miRNA and osteogenic genes. For qRT-PCR analysis of miR-542-3p, TaqMan microRNA reverse transcription kit and a TaqMan microRNA assay kit (Applied Biosystems, Foster City, CA, USA) were used. Whole RNA was isolated from mice calvarial osteoblast using Trizol and cDNA was constructed through reverse transcription. cDNA samples were used as template for real-time PCR for the validation of miRNA. Briefly, the reaction master mix containing 10 $\times$ RT buffer, 5 $\times$ RT primers, MultiScribe reverse transcriptase, RNase inhibitor, 100 mM dNTPs and nuclease-free water was mixed with 20 ng of total RNA. The mixtures were incubated for 30 min at 16 °C, 30 min at 42 °C and 5 min at 85 °C. The PCR was done using 10 μl of PCR master mix containing TaqMan 2 $\times$ Universal PCR Master Mix, 20 $\times$ TaqMan MicroRNA Assay Mix (Applied Biosystems) and the RT products in a volume of 20 μl. The reaction mixtures were incubated in a 96-well plate at 95 °C for 10 min followed by 40 cycles of 95 °C for 15 s and at 60 °C for 1 min using the StepOnePlus Real-Time PCR system (Applied Biosystems). The mean C_t values of each sample were determined from triplicate reactions. The relative expression level of miRNA examined was calculated by $\log_2|2^{-DC_t}|$, in which DC_t was defined as the subtraction of the C_t value of the target miRNA from the C_t value of internal control U6.

For qRT-PCR analysis of osteogenic genes, total RNA was extracted from the cultured cells using Trizol (Life Technologies). cDNA was synthesized from 2 μg total RNA with the Revert AidTM H Minus first strand cDNA synthesis kit (Fermentas, Hanover, MD, USA). SYBR green chemistry was used for quantitative determination of the mRNAs for RUNX-2, BMP-2, Type 1 collagen, Osterix, OCN, BMP-7 and GAPDH following an optimized protocol. The design of sense and antisense oligonucleotide primers was based on published cDNA sequences using the Universal probe library (Roche Diagnostics, USA). Sequences of the primers are given in Supplementary Table S1. For real-time PCR, cDNA was amplified with Light Cycler 480 (Roche Diagnostics, Indianapolis, IN, USA). The temperature profile of the reaction was 95 °C for 5 min, 40 cycles of denaturation at 94 °C for 2 min and annealing and extension at 62 °C for 30 s, extension at 72 °C for 30 s. GAPDH was used to normalize differences in RNA isolation, RNA degradation and the efficiencies of the reverse transcription.

Transfection assay and ALP measurement. Double-stranded RNA oligos representing mature sequences that mimic endogenous miRNAs of miR-542-3p and miRNA negative control (Ambion) were transfected into mice osteoblast cells at 30–50% confluence at 50 nM concentration with Oligofectamine (Invitrogen). Cells were harvested 48 h after transfection for measuring ALP activity and mRNA analysis.

For ALP assay, osteoblasts (mice and human OB) were plated in 96-well (2000 cells/well) plates in growth medium with 10 mM β-glycerophosphate and 50 μg/ml ascorbic acid and incubated for 48 h. After induction, total ALP activity was determined using p-nitrophenylphosphate as substrate and quantified colorimetrically at 405 nm.

Mineralization assay. For mineralization studies, mice calvarial osteoblast cells were isolated and cultured according to a previously published protocol from our laboratory.[34–36] In brief, 2.5×10^3cells/well were seeded in differentiation media with 10% FCS. Cells were transfected with miRNAs and cultured for 21 days at 37 °C in a humidified atmosphere of 5% CO_2 and 95% air, and the medium was changed every 48 h. After 21 days, attached cells were fixed in 4% formaldehyde for 20 min at room temperature and rinsed once in PBS. After fixation, the specimens were processed for staining with 40 mM alizarin red S, which stains areas rich in nascent calcium.

For quantification of alizarin red-S staining, 800 μl of 10% (v/v) acetic acid was added to each well, and plates were incubated at room temperature for 30 min with shaking. The monolayer, now loosely attached to the plate, was then scraped with a cell scraper and transferred with 10% (v/v) acetic acid to a 1.5 ml tube. After vortexing for 30 s, the slurry was overlaid with 500 μl mineral oil (Sigma-Aldrich, St. Louis, MO, USA), heated to exactly 85 °C for 10 min, and transferred to ice for 5 min. The slurry was then centrifuged at 20 000 $\times$ g for 15 min and 500 μl of the supernatant was removed to a new tube. Then 200 μl of 10% (v/v) ammonium hydroxide was added to neutralize the acid. OD (405 nm) of 150-μl aliquots of the supernatant were measured in 96-well format using opaque-walled, transparent-bottomed plates.

Luciferase reporter assay. Primary osteoblast cells, were grown to 85–90% confluence in α-MEM (Sigma-Aldrich) supplemented with 10% FBS, 1% nonessential amino acids, L-glutamine and penicillin/streptomycin at 37 °C under 5% CO_2. Cells were transfected with 200 ng pEZX-MT01 vector in which wild type or mutant form of 3′ UTR of BMP-7 were cloned (contained firefly luciferase as the reporter gene controlled by SV40 promoter gene and reneilla luciferase as the tracking gene controlled by CMV promoter) for 6 h in reduced serum and antibiotics-free OptiMEM with oligofectamine 2000. Cells were co-transfected with the mimic miR-542-3p or a negative control (miR control) (Applied Biosystems) at concentrations of 50 nM. Firefly and Renilla luciferase were measured in cell lysates using a Dual-Luciferase Reporter Assay System (Promega, Madison, WI, USA) on a FLUOstar galaxy (BMG Lab technologies, Melville, NY, USA). Firefly luciferase activity was used for normalization and as an internal control for transfection efficiency.

***In vivo* study.** The study was conducted in accordance with current legislation on animal experiments (Institutional Animal Ethical Committee) at Central Drug Research Institute (CDRI). Six-week-old female Balb/c mice were used in all experiments. These were randomly divided in six groups and underwent either sham operation or bilateral Ovx under general anesthesia by the dorsal approach. These mice received miRNA inhibitor of miR-542-3p or control miC on days 1–3 of first and fourth week, at a dose of 7 mg/kg body weight or a comparable volume of PBS (0.2 ml) through tail vein injection. Six weeks after the first injection, mice were euthanized and blood was taken by dorsal aortic puncture. Serum was collected and stored at -70 °C until analysis. Bone samples were collected for analyses of static and dynamic histomorphometry and biomechanical properties.

Micro-CT analysis. Micro-CT experiments were carried out using Sky Scan 1076 CT scanner (Aartselaar, Antwerp, Belgium) as previously reported.[38–40] Briefly femora and tibiae were dissected from the animals after they were killed, cleaned of soft tissue and fixed before storage in alcohol. X-ray source was set at 70 kV and 100 mA and trabecular region of bone samples were scanned at a nominal resolution (pixels) of 18 mm. A hundred projections were acquired over an angular range of 180°. Then image slices were reconstructed using a modified Feldkamp algorithm using the Sky Scan Nrecon software, which facilitates network distributed reconstruction carried out on personal computer running simultaneously. Parameters like fractional bone volume (bone volume per tissue volume, BV/TV), trabecular number (Tb.N), trabecular thickness (Tb.Th.) and separation (Tb.Sp) were calculated.

BFR/MAR measurements. Dynamic histomorphometric study using double fluorochrome labeling (tetracycline and calcein) of bones was performed following a previously described protocol.[18,34,40] Briefly bones were embedded in an acrylic material for the determination of BFR/bone surface (BFR/BS) and MAR. Fifty

micrometer sections were made using Isomet Bone cutter. Calculations were done for BFR/BS and MAR according to a previously described method.[41]

Bone mechanical strength. Bone mechanical strength was examined by three-point bending strength of femur mid-diaphysis and compressive strength of the fifth lumbar vertebrae using Bone strength tester Model TK 252C as reported earlier.[34]

Western blot analysis. Cells were grown to 60–70% confluence following which they were transfected with miC, miR-542-3p and anti-miR-542-3p and cultured for 48 h. Cells were lysed in mammalian cell lysis buffer (Sigma-Aldrich) with protease inhibitor cocktail (Sigma-Aldrich). Cell lysate was centrifuged at 12 000 *g* for 15 min and supernatant collected. Estimation of protein concentration was determined by Bradford assay. Thirty micrograms of total protein was then resolved by 10% SDS-PAGE gel. After electrophoresis, proteins were transferred onto PVDF membranes (Immobilon-P, Millipore, Billerica, MA, USA). The membranes were probed with BMP-7, Akt, p-Akt, Survivin, p-Survivin, caspase and β-Actin antibodies (Cell Signaling Technology, Danvers, MA, USA) and then incubated with secondary antibodies conjugated with HRP (Cell Signaling Technology). Immunodetection was done using an enhanced chemiluminescence kit (GE Healthcare, Little Chalfont, UK) using Image Quant LAS 4000 (GE Healthcare). Densitometry of blots was done using quantity 1D analysis software and gel doc imaging system.

Analysis of apoptosis by annexin-PI staining. For apoptosis study, osteoblast cells were grown to $\sim$50–60% confluency, serum was withdrawn from the culture for 2 h and then exposed to miRC (50 nM), miR-542-3p(50 nM) and anti-miR-542-3p (20 nM) for 24 h in α-MEM containing 0.5% FCS. Annexin-PI staining for FACS analyses was carried out according to Kit manufacturer's instructions.

Statistical analysis. Data are expressed as mean $\pm$ S.E.M. The data obtained in experiments with multiple treatments were subjected to one-way ANOVA followed by Newman–Keuls test of significance using Prism version 3.0 software. Student's *t*-test was used to study statistical significance in experiments with only two treatments.

Conflict of Interest

The authors declare no conflict of interest.

Acknowledgements. Fellowship grants from the Council of Scientific and Industrial Research (JK, KS, MNM, AMT and AR), Department of Biotechnology (MD), Government of India are acknowledged. Supporting grants: Centre for Research in Anabolic Skeletal Targets in Health and Illness (ASTHI), Council of Scientific and Industrial Research, Department of Biotechnology (DBT), Department of Science and Technology (DST), Government of India. CDRI Communication number: 8604.

Author contributions

Experiments were conceived and designed by DS and JK. JK performed the experiments and analyzed the data. DS wrote the paper. MD and AMT performed the experiments and helped in the analysis of the data. AG, RM and AR synthesized Medicarpin. RT edited the manuscript. KS and MNM analyzed the data. All authors have read and approved of the manuscript before submission.

1. Eskildsen T, Taipaleenmaki H, Stenvang J, Abdallah BM, Ditzel N, Nossent AY *et al.* MicroRNA-138 regulates osteogenic differentiation of human stromal (mesenchymal) stem cells in vivo. *Proc Natl Acad Sci USA* 2011; **108**: 6139–6144.
2. Dong J, Cui X, Jiang Z, Sun J. MicroRNA-23a modulates tumor necrosis factor-alpha-induced osteoblasts apoptosis by directly targeting Fas. *J Cell Biochem* 2013; **114**: 2738–2745.
3. Hassan MQ, Maeda Y, Taipaleenmaki H, Zhang W, Jafferji M, Gordon JA *et al.* miR-218 directs a Wnt signaling circuit to promote differentiation of osteoblasts and osteomimicry of metastatic cancer cells. *J Biol Chem* 2012; **287**: 42084–42092.
4. Hu R, Li H, Liu W, Yang L, Tan YF, Luo XH. Targeting miRNAs in osteoblast differentiation and bone formation. *Expert Opin Ther Targets* 2010; **14**: 1109–1120.
5. Inose H, Ochi H, Kimura A, Fujita K, Xu R, Sato S *et al.* A microRNA regulatory mechanism of osteoblast differentiation. *Proc Natl Acad Sci USA* 2009; **106**: 20794–20799.
6. Li H, Xie H, Liu W, Hu R, Huang B, Tan YF *et al.* A novel microRNA targeting HDAC5 regulates osteoblast differentiation in mice and contributes to primary osteoporosis in humans. *J Clin Invest* 2009; **119**: 3666–3677.
7. Dong S, Yang B, Guo H, Kang F. MicroRNAs regulate osteogenesis and chondrogenesis. *Biochem Biophys Res Commun* 2012; **418**: 587–591.
8. Bae Y, Yang T, Zeng HC, Campeau PM, Chen Y, Bertin T *et al.* miRNA-34c regulates Notch signaling during bone development. *Hum Mol Genet* 2012; **21**: 2991–3000.
9. Gao J, Yang T, Han J, Yan K, Qiu X, Zhou Y *et al.* MicroRNA expression during osteogenic differentiation of human multipotent mesenchymal stromal cells from bone marrow. *J Cell Biochem* 2011; **112**: 1844–1856.
10. Guo J, Ren F, Wang Y, Li S, Gao Z, Wang X *et al.* miR-764-5p promotes osteoblast differentiation through inhibition of CHIP/STUB1 expression. *J Bone Miner Res* 2012; **27**: 1607–1618.
11. Taipaleenmaki H, Bjerre Hokland L, Chen L, Kauppinen S, Kassem M. Mechanisms in endocrinology: micro-RNAs: targets for enhancing osteoblast differentiation and bone formation. *Eur J Endocrinol* 2012; **166**: 359–371.
12. Li Z, Hassan MQ, Volinia S, van Wijnen AJ, Stein JL, Croce CM *et al.* A microRNA signature for a BMP2-induced osteoblast lineage commitment program. *Proc Natl Acad Sci USA* 2008; **105**: 13906–13911.
13. Huang J, Zhao L, Xing L, Chen D. MicroRNA-204 regulates Runx2 protein expression and mesenchymal progenitor cell differentiation. *Stem Cells* 2010; **28**: 357–364.
14. Itoh T, Nozawa Y, Akao Y. MicroRNA-141 and $-$200a are involved in bone morphogenetic protein-2-induced mouse pre-osteoblast differentiation by targeting distal-less homeobox 5. *J Biol Chem* 2009; **284**: 19272–19279.
15. Zhang J, Tu Q, Bonewald LF, He X, Stein G, Lian J *et al.* Effects of miR-335-5p in modulating osteogenic differentiation by specifically downregulating Wnt antagonist DKK1. *J Bone Miner Res* 2011; **26**: 1953–1963.
16. Itoh T, Takeda S, Akao Y. MicroRNA-208 modulates BMP-2-stimulated mouse preosteoblast differentiation by directly targeting V-ets erythroblastosis virus E26 oncogene homolog 1. *J Biol Chem* 2010; **285**: 27745–27752.
17. Sato MM, Nashimoto M, Katagiri T, Yawaka Y, Tamura M. Bone morphogenetic protein-2 down-regulates miR-206 expression by blocking its maturation process. *Biochem Biophys Res Commun* 2009; **383**: 125–129.
18. Bhargavan B, Singh D, Gautam AK, Mishra JS, Kumar A, Goel A *et al.* Medicarpin, a legume phytoalexin, stimulates osteoblast differentiation and promotes peak bone mass achievement in rats: evidence for estrogen receptor beta-mediated osteogenic action of medicarpin. *J Nutr Biochem* 2012; **23**: 27–38.
19. Oneyama C, Morii E, Okuzaki D, Takahashi Y, Ikeda J, Wakabayashi N *et al.* MicroRNA-mediated upregulation of integrin-linked kinase promotes Src-induced tumor progression. *Oncogene* 2012; **31**: 1623–1635.
20. Yoon S, Choi YC, Lee S, Jeong Y, Yoon J, Baek K. Induction of growth arrest by miR-542-3p that targets survivin. *FEBS Lett* 2010; **584**: 4048–4052.
21. Chen D, Zhao M, Mundy GR. Bone morphogenetic proteins. *Growth Factors* 2004; **22**: 233–241.
22. Gautschi OP, Frey SP, Zellweger R. Bone morphogenetic proteins in clinical applications. *ANZ J Surg* 2007; **77**: 626–631.
23. Zhu W, Rawlins BA, Boachie-Adjei O, Myers ER, Arimizu J, Choi E *et al.* Combined bone morphogenetic protein-2 and -7 gene transfer enhances osteoblastic differentiation and spine fusion in a rodent model. *J Bone Miner Res* 2004; **19**: 2021–2032.
24. ten Dijke P, Korchynskyi O, Valdimarsdottir G, Goumans MJ. Controlling cell fate by bone morphogenetic protein receptors. *Mol Cell Endocrinol* 2003; **211**: 105–113.
25. Shimizu T, Kayamori T, Murayama C, Miyamoto A. Bone morphogenetic protein (BMP)-4 and BMP-7 suppress granulosa cell apoptosis via different pathways: BMP-4 via PI3K/PDK-1/Akt and BMP-7 via PI3K/PDK-1/PKC. *Biochem Biophys Res Commun* 2012; **417**: 869–873.
26. Belyanskaya LL, Hopkins-Donaldson S, Kurtz S, Simoes-Wust AP, Yousefi S, Simon HU *et al.* Cisplatin activates Akt in small cell lung cancer cells and attenuates apoptosis by survivin upregulation. *Int J Cancer* 2005; **117**: 755–763.
27. Yang S, Lim M, Pham LK, Kendall SE, Reddi AH, Altieri DC *et al.* Bone morphogenetic protein 7 protects prostate cancer cells from stress-induced apoptosis via both Smad and c-Jun NH2-terminal kinase pathways. *Cancer Res* 2006; **66**: 4285–4290.
28. Wang J, Jin Y, Xu Z, Zheng Z, Wan S. Involvement of caspase-3 activity and survivin downregulation in cinobufocini-induced apoptosis in A 549 cells. *Exp Biol Med (Maywood)* 2009; **234**: 566–572.
29. Zhang X, Xie X, Heckmann BL, Saarinen AM, Czyzyk TA, Liu J. Target disruption of G0/G1 Switch Gene 2 enhances adipose lipolysis, alters hepatic energy balance, and alleviates high fat diet-induced liver steatosis. *Diabetes* 2013; e-pub ahead of print 5 November 2013; doi:10.2337/db13-1422.
30. Chen G, Deng C, Li YP. TGF-beta and BMP signaling in osteoblast differentiation and bone formation. *Int J Biol Sci* 2012; **8**: 272–288.
31. Cao X, Chen D. The BMP signaling and in vivo bone formation. *Gene* 2005; **357**: 1–8.
32. Lechler P, Schaumburger J, Kock FX, Balakrishnan S, Doukas S, Prantl L *et al.* The oncofetal gene survivin promotes cell proliferation and survival in primary human osteoblastic cells. *Calcif Tissue Int* 2011; **89**: 211–220.

33. Jee WS, Yao W. Overview: animal models of osteopenia and osteoporosis. *J Musculoskelet Neuronal Interact* 2001; **1**: 193–207.
34. Bhargavan B, Gautam AK, Singh D, Kumar A, Chaurasia S, Tyagi AM *et al.* Methoxylated isoflavones, cajanin and isoformononetin, have non-estrogenic bone forming effect via differential mitogen activated protein kinase (MAPK) signaling. *J Cell Biochem* 2009; **108**: 388–399.
35. Gautam AK, Bhargavan B, Tyagi AM, Srivastava K, Yadav DK, Kumar M *et al.* Differential effects of formononetin and cladrin on osteoblast function, peak bone mass achievement and bioavailability in rats. *J Nutr Biochem* 2011; **22**: 318–327.
36. Trivedi R, Kumar S, Kumar A, Siddiqui JA, Swarnkar G, Gupta V *et al.* Kaempferol has osteogenic effect in ovariectomized adult Sprague-Dawley rats. *Mol Cell Endocrinol* 2008; **289**: 85–93.
37. Tyagi AM, Gautam AK, Kumar A, Srivastava K, Bhargavan B, Trivedi R *et al.* Medicarpin inhibits osteoclastogenesis and has nonestrogenic bone conserving effect in ovariectomized mice. *Mol Cell Endocrinol* 2010; **325**: 101–109.
38. Tyagi AM, Srivastava K, Mansoori MN, Trivedi R, Chattopadhyay N, Singh D. Estrogen deficiency induces the differentiation of IL-17 secreting Th17 cells: a new candidate in the pathogenesis of osteoporosis. *PLoS One* 2012; **7**: e44552.
39. Tyagi AM, Srivastava K, Kureel J, Kumar A, Raghuvanshi A, Yadav D *et al.* Premature T cell senescence in Ovx mice is inhibited by repletion of estrogen and medicarpin: a possible mechanism for alleviating bone loss. *Osteoporos Int* 2012; **23**: 1151–1161.
40. Pandey R, Gautam AK, Bhargavan B, Trivedi R, Swarnkar G, Nagar GK *et al.* Total extract and standardized fraction from the stem bark of Butea monosperma have osteoprotective action: evidence for the nonestrogenic osteogenic effect of the standardized fraction. *Menopause* 2010; **17**: 602–610.
41. Hara K, Kobayashi M, Akiyama Y. Vitamin K2 (menatetrenone) inhibits bone loss induced by prednisolone partly through enhancement of bone formation in rats. *Bone* 2002; **31**: 575–581.

Cell Death and Disease **is an open-access journal published by** ***Nature Publishing Group*****. This work is licensed under a Creative Commons Attribution-NonCommercial-NoDerivs 3.0 Unported License. To view a copy of this license, visit http://creativecommons.org/licenses/by-nc-nd/3.0/**

Supplementary Information accompanies this paper on Cell Death and Disease website (http://www.nature.com/cddis)